Journal of Solid State Chemistry 185 (2012) 180–186

Contents lists available at SciVerse ScienceDirect

Journal of Solid State Chemistry

journal homepage: www.elsevier.com/locate/jssc

[La(UO$_2$)V$_2$O$_7$][(UO$_2$)(VO$_4$)] the first lanthanum uranyl-vanadate with structure built from two types of sheets based upon the uranophane anion-topology

A. Mer, S. Obbade [1], M. Rivenet, C. Renard *, F. Abraham

Univ. Lille Nord de France, Unité de Catalyse et de Chimie du Solide, UCCS UMR CNRS 8181, ENSCL-USTL, B.P. 90108, 59652 Villeneuve d'Ascq Cedex, France

ARTICLE INFO

Article history:
Received 25 July 2011
Received in revised form
18 October 2011
Accepted 24 October 2011
Available online 11 November 2011

Keywords:
Lanthanum uranyl vanadate
Crystal structure determination
Solid state synthesis

ABSTRACT

The new lanthanum uranyl vanadate divanadate, [La(UO$_2$)V$_2$O$_7$][(UO$_2$)(VO$_4$)] was obtained by reaction at 800 °C between lanthanum chloride, uranium oxide (U$_3$O$_8$) and vanadium oxide (V$_2$O$_5$) and the structure was determined from single-crystal X-ray diffraction data. This compound crystallizes in the orthorhombic system with space group $P2_12_12_1$ and unit-cell parameters $a=6.9470(2)$ Å, $b=7.0934(2)$ Å, $c=25.7464(6)$ Å, $V=1268.73(5)$ Å^3, $Z=4$. A full matrix least-squares refinement yielded $R_1=0.0219$ for 5493 independent reflections. The crystal structure is characterized by the stacking of uranophane-type sheets $^2_\infty[(UO_2)(VO_4)]^-$ and double layers $^2_\infty[La(UO_2)(V_2O_7)]^+$ connected through La–O bonds involving the uranyl oxygen of the uranyl-vanadate sheets. The double layers result from the connection of two $^2_\infty[La(UO_2)(VO_4)_2]^-$ sheets derived from the uranophane anion-topology by replacing half of the uranyl ions by lanthanum atoms and connected through the formation of divanadate entities.

1. Introduction

The chemistry of actinides, and in particular of uranium, has attracted a renewal of interest these last two decades with the improvement of reprocessing and assessment of nuclear waste disposal. In this connection the crystal chemistry of inorganic compounds containing uranyl has received considerable attention and reveals an important diversity, either in minerals or in synthesized compounds [1]. In particular, the association of uranyl ion and various inorganic oxoanions such as vanadate, phosphate, silicate, niobate, molybdate, etc., generates a vast number of structures with varied architectures and dimensionalities. This large structural diversity results from the numerous possible linkages between the different uranium polyhedra which can be hexagonal bipyramid, pentagonal bipyramid or square bipyramids and the various inorganic oxoanion geometries which can be tetrahedron, square pyramid, trigonal bipyramid or octahedron, depending upon the nature of the post transition element (Si, P, As) or transition metal in its highest possible oxidation states (V, Nb, Mo, W, etc.).

A part of interest of our group of research focuses on the solid state chemistry of uranyl-vanadates compounds [2]. Uranyl-vanadates comprise perhaps the most insoluble of uranyl minerals [3], which is one of the reasons why they are so abundant in nature. The natural uranyl-vanadate species the most represented are the carnotite K$_2$[(UO$_2$)$_2$V$_2$O$_8$]·3H$_2$O [4], the tyuyamunite Ca[(UO$_2$)$_2$V$_2$O$_8$]·5–8H$_2$O [5], the Francevillite (Ba,Pb)[(UO$_2$)$_2$V$_2$O$_8$]·5H$_2$O [6] and the sengierite Cu$_2$[(UO$_2$)$_2$V$_2$O$_8$](OH)$_2$·6H$_2$O [7]. Their structures consist on uranyl-vanadate francevillite-type sheets $^2_\infty[(UO_2)_2(VO_4)_2]^{2-}$ built from UO$_7$ pentagonal bipyramids bridged by centrosymmetric $[V_2O_8]^{6-}$ units formed from two inverse VO$_5$ square pyramids sharing an edge. In most of the compounds, the interlayer space is occupied by monovalent or divalent ions and H$_2$O molecules but trivalent aluminium can also be found in a few mineral compounds such as vanuralite Al[(UO$_2$)$_2$V$_2$O$_8$](OH)·11H$_2$O [8] or metavanuralite Al[(UO$_2$)$_2$V$_2$O$_8$](OH)·8H$_2$O [8]. Synthetic compounds $M^{n+}_{2/n}$[(UO$_2$)$_2$V$_2$O$_8$]·xH$_2$O based on the uranyl-vanadate francevillite-type sheet have been reported where M^{n+} is an alkaline metal [9], NH_4^+ [10] or Ag^+ [11], an alkaline earth [12,13] or a divalent transition metal [12,14] or an organic template [15]. Other synthetic layered compounds with formula (UO$_2$)$_3$(VO$_4$)$_2$·5H$_2$O [16], M_6(UO$_2$)$_5$(VO$_4$)$_2$O$_5$ with M=Na, K [17] and Rb [18], CsUV$_3$O$_{11}$ [19], Cs$_4$[(UO$_2$)$_2$(V$_2$O$_7$)O$_2$] [20] were obtained and characterized. Although layered compounds predominate due to the presence of uranyl ions that preclude the connection in the third direction, three dimensional uranyl-vanadate arrangements were synthesized in the presence of small monovalent cations Li^+, Na^+ or Ag^+ [21] or using protonated amines as structure directing agents [22].

* Corresponding author. Fax: +33 3 20 43 68 14.
E-mail address: catherine.renard@ensc-lille.fr (C. Renard).
[1] Present address: PHELMA, MINATEC, Bureau M403, 3 Parvis Louis Néel, BP 257, 38016 Grenoble Cedex 01, France.

0022-4596/$ - see front matter © 2011 Elsevier Inc. All rights reserved.
doi:10.1016/j.jssc.2011.10.042

Although the rare earths are found as impurities in some uraninite ores, no uranyl vanadate minerals containing rare earths was reported up today, to our knowledge. However, rare earths constitute an important part of fission products and some of them share sometimes similar physicochemical properties with transuranium elements at the oxidation degree (III). This similarity is an asset used to simulate the behaviour of minor actinides included in the nuclear wastes for deep underground disposal, which is a critical issue in the management of spent fuel. The alteration products of the nuclear waste in wet and oxidizing conditions are the phases containing the uranyl ion resulting from the oxidation of uranium U^{4+} in U^{6+}, which can be associated with different oxoanions (phosphates, vanadates, arsenates, etc.) and some radionuclides (fission products and actinides). The knowledge of the different compounds likely to form is therefore an important purpose but the number of studies dedicated to rare earths uranyl vanadate phases remains very low since only two papers report the synthesis of layered hydrated compounds $Ln(UVO_6)_3 \cdot nH_2O$ [23,24].

As a part of our ongoing research on new uranyl-vanadates we are studying the synthesis of lanthanide uranyl-vanadates. In this paper, we report the synthesis and structure of the first anhydrous lanthanum uranyl-vanadate with a framework constituted by the stacking of two different uranophane-type layers.

2. Experimental

2.1. Synthesis

Single crystals of $[La(UO_2)V_2O_7][(UO_2)(VO_4)]$ were obtained by solid state reaction between lanthanum chloride $LaCl_3 \cdot 7H_2O$ and $U_2V_2O_{11}$ used as a precursor of uranium and vanadium mixed in the molar ratio corresponding to Ln/U/V=1/3/3. The mixture was heated in air at 870 °C for 10 h in a platinum crucible and cooled to ambient temperature for 20 h.

Pure polycrystalline sample of $[La(UO_2)V_2O_7][(UO_2)(VO_4)]$ was prepared by conventional solid-state reaction, using pure initial materials $LaCl_3 \cdot 7H_2O$ (Sigma), U_3O_8 (Prolabo), and V_2O_5 (Aldrich) according to the following reaction:

$$2/3U_3O_8 + 3/2V_2O_5 + LaCl_3 + 13/12O_2 \rightarrow LaU_2V_3O_{15} + 3/2Cl_2$$

The homogeneous mixture was slowly heated up to 800 °C in a platinum crucible and maintained at this temperature for 2 weeks with intermediate grindings after cooling at room temperature. The X-ray diffraction pattern of the powder is identical to that of crushed single crystals and to that of the calculated pattern from the crystal structure results. For unit cell parameters determination a X-ray diffraction pattern was recorded under air over the angular range of 5–80° (2θ), with a step length of 0.02° (2θ) and a counting time of 15 s $step^{-1}$ with a Bruker AXS D8 ADVANCE diffractometer with the parafocusing Bragg–Brentano geometry, using Cu$K\alpha$1, α2 radiation ($\lambda_{K\alpha1}$ = 1.54051 Å, $\lambda_{K\alpha2}$ = 1.54433 Å) and an energy dispersive detector (sol-X). Unit cell parameters were refined to a=6.9448(1), b=7.0885(1), c=25.7462(6) Å by applying the "pattern matching" option of the FullProf program [25] to the whole diagram. The peak shape was fitted by a pseudo-Voigt function. In order to describe the angular dependence of the peak full-width at half-maximum (H), the formula of Caglioti et al. [26] was used, where U, V and W are parameters refined in the process. The calculations involved the refinement of 2θ zero-point, cell parameters and background level by a polynomial function. The fit of calculated data with regard to the observed data was indicated by the reliability factors and by the plot of observed and calculated patterns represented in Fig. 1.

In spite of numerous tentative by varying the lanthanide metal, the starting materials and the experimental conditions (temperature, duration, etc.) no other lanthanide uranyl-vanadate could be synthesized by the solid state reaction. In fact $LnVO_4$ is preliminarily formed and does not further react.

2.2. Single-crystal X-ray diffraction and structure determination

A well-shaped yellow crystal of $[La(UO_2)V_2O_7][(UO_2)(VO_4)]$ was selected for X-ray diffraction investigations. Single-crystal X-ray diffraction data were collected on a Bruker X8-APEX2 X-ray diffractometer equipped with a 4K CCD detector and monochromated Mo$K\alpha$ radiation (λ=0.7107 Å).

Details of the data collection are given in Table 1. Before the crystal structure determination, the intensity data were corrected for Lorentz, polarization and background effects using Bruker program SAINT [27]. Then the absorption corrections were computed by the Gaussian face-indexed method with the shape of the

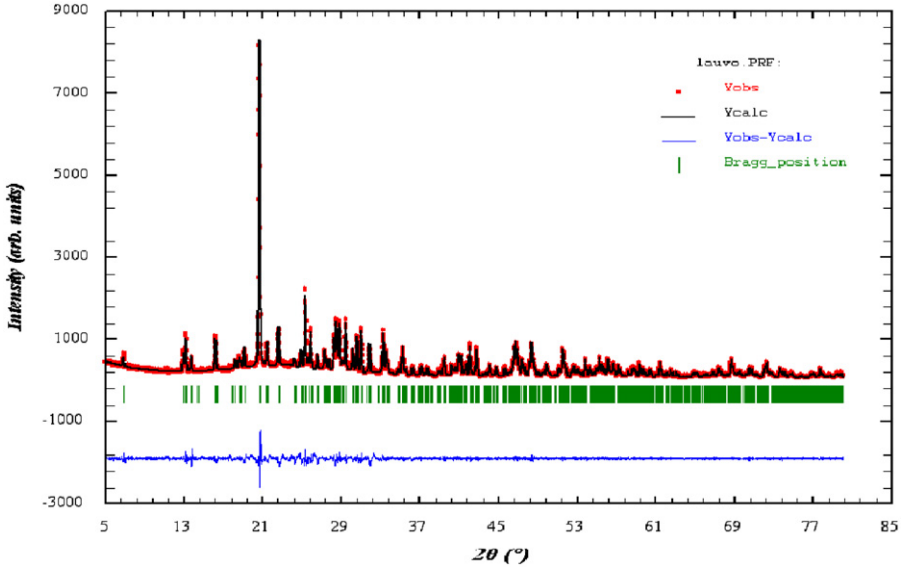

Fig. 1. Observed (red), calculated (black) XRD patterns and their difference (blue) for $[La(UO_2)V_2O_7][(UO_2)(VO_4)]$. (For interpretation of the references to colour in this figure legend, the reader is referred to the web version of this article.)

crystal using the program XPREP of the SHELXTL package [28], followed by a semi-empirical correction based on redundancy using the SADABS program [29].

Table 1
Crystal data, intensity collection and structure refinement parameters for $[La(UO_2)V_2O_7][(UO_2)(VO_4)]$.

Crystal data	
Crystal symmetry	Orthorhombic
Space group	$P2_12_12_1$
Unit-cell refined from single-crystal data	$a=6.9470(2)$ Å
	$b=7.0934(2)$ Å
	$c=25.7464(6)$ Å
Unit-cell volume	$V=1268.73(5)$ Å^3
Z	4
Calculated density	5.276 g/cm^3
Colour	Yellow
Data collection	
Temperature (K)	296(2)
Equipment	Bruker APEX
Radiation Mo($K\alpha$)	0.71073 Å
Scan mode	φ and ω
Recording angular range (deg.)	2.98/34.84
Recording reciprocal space	$-11 \le h \le 10$
	$-11 \le k \le 11$
	$-41 \le l \le 40$
Number of reflections	
Measured/independent	52,343/5492
Absorption μ	30.925
Refinement	
Refined parameters/restraints	191/0
Goodness of fit on F^2	0.989
R_1 [$I > 2$sigma(I)]	0.0219
wR_2 [$I > 2$sigma(I)]	0.0339

Note: $R1=\Sigma(|F_0|-|F_c|)/\Sigma|F_0|$; $wR_2=[\Sigma_w(F_0^2-F_c^2)^2/\Sigma_w(F_0^2)^2]1/2$; $w=1/[\sigma^2(F_0^2)+(aP)^2+bP]$ where a and b are refinable parameters and $P=(F_0^2+2F_c^2)/3$.

The crystal structure of $[La(UO_2)V_2O_7][(UO_2)(VO_4)]$ was solved in the non-centrosymmetric $P2_12_12_1$ space group by means of direct methods strategy using SHELXS program [28] that localize the heavy atoms U, La and V. The positions of the oxygen atoms were deduced from subsequent refinements and difference Fourier syntheses. Refinement of atomic positional parameters, anisotropic displacement parameters for U, La, V and O atoms yielded the final $R=0.0219$ and $R_w=0.0339$. The atomic positions and the equivalent isotropic displacement factors are given in Table 2.

Table 2
Atomic positions, equivalent isotropic displacement parameters U_{eq} (Å^2) for $La[(UO_2)V_2O_7][(UO_2)(VO_4)]$.

Atom	Site	Occ.	x	y	z	U_{eq}
U(1)	4a	1	0.16619(2)	0.86861(2)	0.99860(1)	0.00639(3)
U(2)	4a	1	0.59762(2)	0.13113(2)	1.17437(1)	0.00759(3)
La(1)	4a	1	0.34948(3)	0.63273(4)	1.14491(1)	0.00813(4)
V(1)	4a	1	0.81511(9)	0.62811(11)	0.17749(3)	0.00790(12)
V(2)	4a	1	0.13757(9)	0.13198(11)	1.19441(3)	0.00814(12)
V(3)	4a	1	0.18428(10)	0.41508(9)	1.01787(3)	0.00717(14)
O(1)	4a	1	0.1015(4)	0.8575(5)	0.93065(10)	0.01208(6)
O(2)	4a	1	0.6602(5)	0.8145(4)	1.17270(13)	0.01341(6)
O(3)	4a	1	0.2281(4)	0.8573(5)	1.06676(11)	0.01084(5)
O(4)	4a	1	0.5629(4)	0.1182(5)	1.10675(11)	0.01666(6)
O(5)	4a	1	0.6252(4)	0.1374(5)	1.24369(11)	0.01584(6)
O(6)	4a	1	0.6562(5)	0.4466(4)	1.16691(12)	0.01405(9)
O(7)	4a	1	−0.0676(4)	0.1376(5)	1.16155(10)	0.01365(6)
O(8)	4a	1	0.2894(4)	0.3163(4)	1.18529(13)	0.01175(6)
O(9)	4a	1	0.2916(4)	−0.0486(4)	1.17982(13)	0.01317(6)
O(10)	4a	1	0.0748(4)	0.1129(5)	1.26075(11)	0.02037(7)
O(11)	4a	1	0.1573(4)	0.1907(4)	0.99561(12)	0.01202(6)
O(12)	4a	1	0.9959(4)	0.6361(5)	1.13700(11)	0.01564(6)
O(13)	4a	1	0.3448(4)	0.5745(4)	0.98680(11)	0.00930(5)
O(14)	4a	1	−0.0134(4)	0.5713(4)	1.01514(12)	0.01081(6)
O(15)	4a	1	0.2572(4)	0.4064(4)	1.07867(11)	0.01184(6)

Note: The U_{eq} values are defined by $U_{eq}=1/3(\Sigma_i\Sigma_j U_{ij}a_i^*a_j^*a_ia_j)$.

Table 3
Selected bond distances (Å), angles (deg.) and bond valences for $[La(UO_2)V_2O_7][(UO_2)(VO_4)]$.

U environment								
Atom	d_{U-O}	s_{ij}	**Atom**	d_{U-O}	s_{ij}			
U1–O3	1.809(3)	*1.594*	U2–O4	1.760(3)	*1.752*	***Uranyl ion angle***		
U1–O1	1.808(3)	*1.597*	U2–O5	1.796(3)	*1.634*	O(1)–U(1)–O(3)	174.9(1)	
U1–O11^{i}	2.287(3)	*0.635*	U2–O6	2.282(3)	*0.641*	O(4)–U(2)–O(5)	177.6(1)	
U1–O14^{ii}	2.294(3)	*0.626*	U2–O2^{iv}	2.288(3)	*0.633*			
U1–O13^{iii}	2.300(3)	*0.619*	U2–O7^{v}	2.349(3)	*0.563*	***Divanadate angle***		
U1–O13	2.446(3)	*0.467*	U2–O9	2.483(3)	*0.435*	V(1)–O(10)–V(2)	139.2(2)	
U1–O14	2.487(3)	*0.432*	U2–O8	2.528(3)	*0.399*			
$\sum s_{ij}$		**5.97**	$\sum s_{ij}$		**6.057**			
V environment								
Atom	d_{V-O}	s_{ij}	**Atom**	d_{V-O}	s_{ij}	**Atom**	d_{V-O}	s_{ij}
V1–O12	1.633(3)	*1.583*	V2–O7	1.658(3)	*1.48*	V3–O15	1.647(3)	*1.524*
V1–O2	1.710(3)	*1.286*	V2–O8	1.696(3)	*1.335*	V3–O11	1.702(3)	*1.314*
V1–O6	1.718(3)	*1.258*	V2–O9	1.711(3)	*1.282*	V3–O14	1.766(3)	*1.105*
V1–O10^{vii}	1.768(3)	*1.099*	V2–O10	1.768(3)	*1.099*	V3–O13	1.778(3)	*1.070*
$\sum s_{ij}$		**5.226**	$\sum s_{ij}$		**5.196**	$\sum s_{ij}$		**5.013**
La environment								
Atom	d_{La-O}	s_{ij}						
La1–O15	2.428(3)	*0.501*	La1–O2	2.614(3)	*0.303*			
La1–O9^{i}	2.465(3)	*0.453*	La1–O1^{ii}	2.618(3)	*0.300*			
La1–O12^{vi}	2.465(3)	*0.453*	La1–O3	2.701(3)	*0.239*			
La1–O8	2.509(3)	*0.402*	La1–O5^{viii}	2.874(3)	*0.150*			
La1–O6	2.570(3)	*0.341*						
			$\sum s_{ij}$		**3.142**			

Note: Symmetry codes: (i) x, $1+y$, z; (ii) $0.5+x$, $1.5-y$, $2-z$; (iii) $-0.5+x$, $1.5-y$, $2-z$; (iv) x, $-1+y$, z; (v) $1+x$, y, z; (vi) $-1+x$, y, z; (vii) $1-x$, $0.5+y$, $2.5-z$; (viii) $1-x$, $-0.5+y$, $2.5-z$.

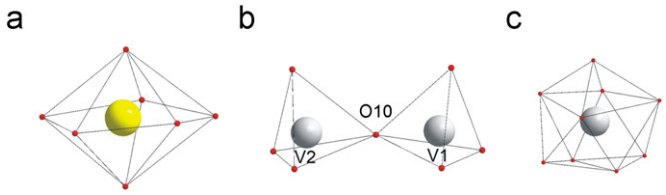

Fig. 2. Uranium (a), vanadium (b) and lanthanum (c) polyhedra in $[La(UO_2)V_2O_7][(UO_2)(VO_4)]$.

2.3. Thermal analysis

Differential Thermal Analysis (DTA) was carried out on $[La(UO_2)V_2O_7][(UO_2)(VO_4)]$ with a SETARAM 92-1600 instrument at a heating rate of 5 °C min^{-1} using platinum crucibles in the range of 20–1200 °C both on heating and cooling.

3. FTIR and Raman spectroscopy

The infrared spectrum was obtained using the KBr dispersion technique (1 mg of sample in 125 mg KBr) with a Bruker Vector 22 FTIR spectrometer, which covers the range of 400–4000 cm^{-1}.

The Raman spectra were obtained at room temperature with the 522.6 nm excitation line from a Spectra Physics krypton ion laser. The beam was focused onto the sample using the microscopic configuration of the apparatus. The scattered light was analysed with a XY800 Raman Dilor spectrometer equipped with an optical multichannel charge coupled device liquid nitrogen-cooled detector. In the 300–1000 cm^{-1} required range, the spectral resolution is approximately 0.5 cm^{-1}.

4. Results and discussion

4.1. Description of structure

Table 3 provides selected metal to oxygen distances, uranyl angles and bond valences calculated using Brese and O'Keeffe [30] data with $b=0.37$ Å except for U–O bonds for which the coordination independent parameters ($R_{ij}=2.051$ Å, $b=0.519$ Å) were taken from Burns et al. [31].

The structure of $[La(UO_2)V_2O_7][(UO_2)(VO_4)]$ contains two symmetrically independent uranium atoms U(1) and U(2) surrounded by seven oxygen atoms forming pentagonal bipyramids (PBP) (Fig. 2a). Each uranium atom is strongly bonded to two oxygen atoms, O(1),O(3) for U(1) and O(5),O(4) for U(2), at short distances ranging from 1.760(3) to 1.809(3) Å, forming a nearly linear uranyl ion UO_2^{2+} (O(1)–U(1)–O(3)=174.9(1)°; O(4)–U(2)–O(5)=177.6(1)°). Each uranyl ion UO_2^{2+} is surrounded in the equatorial plane by five oxygen atoms with U–O bond lengths in the ranges 2.287(3)–2.487(3) Å and 2.282(3)–2.528(3) Å for U(1) and U(2), respectively. Their average values, 2.363 and 2.386 Å, correspond to the mean value of 2.368 Å found for 270 UO_7 polyhedra in 143 structures [1].

There are three independent vanadium atoms V(1), V(2) and V(3), having a strongly distorted tetrahedral coordination (Fig. 2b). The V(1) and V(2) environments are defined by one oxygen atom at a shorter distance (1.633(3) Å and 1.6583(3) Å for V(1)–O(12) and V(2)–O(7), respectively), two atoms (O(2) and O(6) for V(1) and O(8) and O(9) for V(2)) at intermediate and nearly equal distances between 1.696(3) and 1.718(3) Å, and finally O(10) at a longer distance 1.768(3) Å from V(1) and V(2). The O(10) atom is shared between $V(1)O_4$ and $V(2)O_4$ tetrahedra to form a V_2O_7 divanadate unit with a non-linear angle V(1)–O(10)–V(2) of 139.2(2)°. The bridging V–O–V angle in V_2O_7 divanadate units varies from perfectly linear as, for example in $U_2V_2O_{11}$ [32,33] to 122° in $Pb_2V_2O_7$ [34]. For V(3), O(15) is at a short distance, 1.647(3) Å, O(11) at an intermediate distance, 1.702(3) Å and finally O(13) and O(14) at longer distances, 1.778(3) and 1.766(3) Å, respectively.

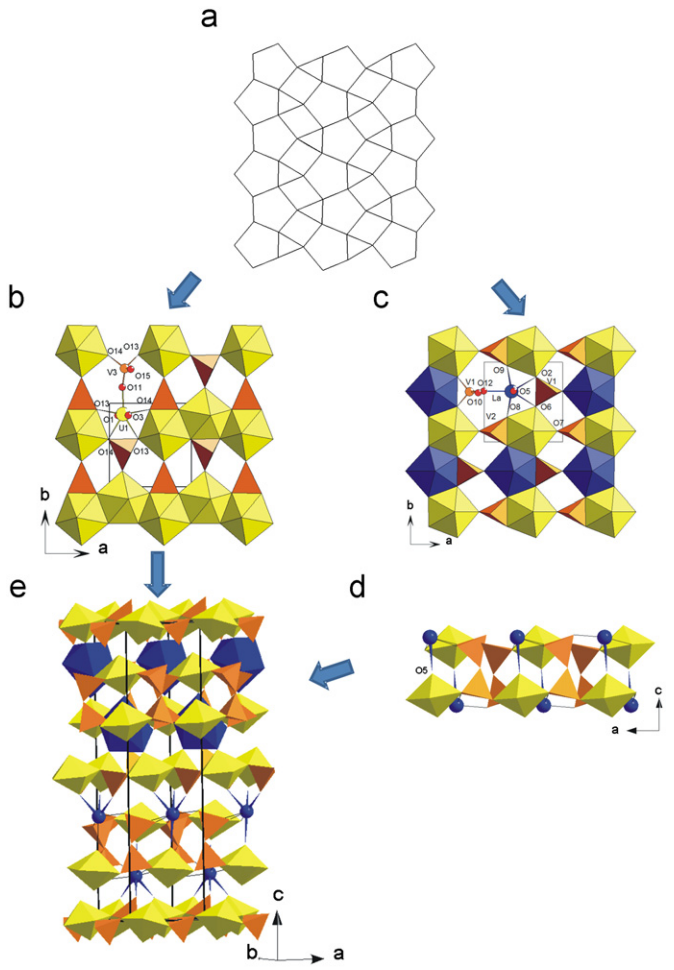

Fig. 3. The uranophane anion-topology (a) with occupation of pentagons by uranyl ions and triangle by vanadate ions to form the sheet $[(UO_2)(VO_4)]^-$ (b) and with occupation of half the pentagons by uranyl ions and half by lanthanum ions to form the sheet $[La(UO_2)(VO_4)_2]^-$ (c) further connected through the formation of divanadate ions to form the double layers $[La(UO_2)(V_2O_7)]^+$ (d). Finally, the three-dimensional structure of $[La(UO_2)V_2O_7][(UO_2)(VO_4)$ results of the stacking of $[(UO_2)(VO_4)]^-$ sheets and $[La(UO_2)(V_2O_7)]^+$ double layers along c (e).

The La atom is surrounded by nine oxygen atoms at distances from 2.428(3) to 2.874(3) Å forming a tricapped trigonal prism (Fig. 2c). The La coordination is perfectly defined, the next La–O distance being 3.822(3) Å.

On the basis of the U–O, V–O and La–O bond lengths, bond valence sums were calculated to be 5.97, 6.06, 5.23, 5.20, 5.01 and 3.14 *vu*, for U(1), U(2), V(1), V(2), V(3) and La, respectively. These values are in agreement with the expected values. Bond valence sums for the O atoms range from 1.75 to 2.22, the lowest values being for uranyl oxygens.

Although the overall structure results from a three-dimensional arrangement of UO_7, LaO_9 and VO_4 polyhedra, it may be instructional in the first instance to consider layers in the (0 0 1) plane, which are further linked in the third dimension along *c*.

For $U(1)O_7$ PBPs the five equatorial oxygen belong to $V(3)O_4$ tetrahedra (Fig. 3b). $U(1)O_7$ PBPs share opposite edges O(13)–O(14)

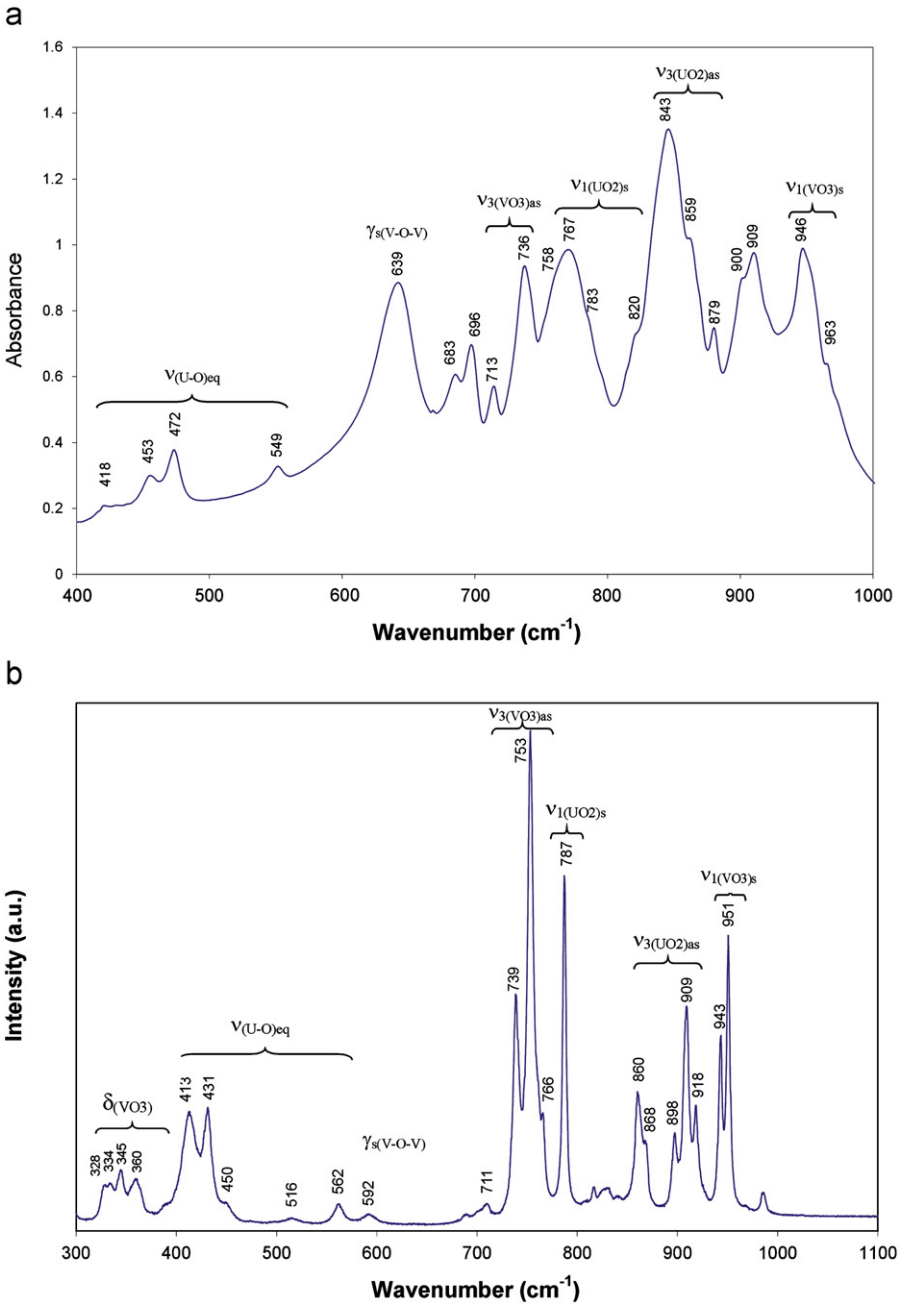

Fig. 4. (a) Infra-red and (b) Raman spectra of $[La(UO_2)V_2O_7][(UO_2)(VO_4)]$.

to form $^1_\infty[UO_5]$ infinite chains extending down the [1 0 0] direction and further connected through $V(3)O_4$ tetrahedra by sharing O(13)–O(14) edges and O(11) vertex to built uranophane-type sheets $^2_\infty[(UO_2)(VO_4)]^-$ parallel to the (0 0 1) plane (Fig. 3b). The uranophane-type sheet $^2_\infty[(UO_2)(VO_4)]^-$ is described from the uranophane anion-topology (Fig. 3a) by the occupation of all the pentagons by uranyl ions when all the triangles correspond to the O(11)–O(13)–O(14) faces of the $V(3)O_4$ tetrahedra. The fourth oxygen atom O(15) of the $V(3)O_4$ tetrahedra points up or down the layers, for all the tetrahedra sharing an edge with PBPs of a $^1_\infty[UO_5]$ chain. On one side it points up (*u*) and on the other side it points down (*d*) giving the *ud* geometric isomer [32]. Similar layers are formed in $(UO_2)_2(V_2O_7)$ [33] but disorientation of the VO_4 tetrahedra gives corrugated layers and allows the connection of the layers in the third direction through the formation of divanadate entities.

For $U(2)O_7$ PBPs the five equatorial oxygen belong to $V(1)O_4$ and $V(2)O_4$ tetrahedra. The $U(2)O_7$ PBPs do not share directly any anion but are connected through $V(2)O_4$ tetrahedra by sharing O(8)–O(9) edges and O(7) corners to form infinite $^1_\infty[(UO_2)O_2(V(2)O_4)]^{5-}$ chains extending down [1 0 0] (Fig. 3c) further connected in the [0 1 0] direction through $V(1)O_4$ tetrahedra by sharing opposite O(2) and O(6) corners with two different $V(1)O_4$ tetrahedra to create sheet $^2_\infty[(UO_2)(VO_4)_2]^{4-}$ similar to that found in $Na_{5.5}(UO_2)_3(H_{0.5}PO_4)(PO_4)_3$ [35] and also deduced from the uranophane anion-topology (Fig. 3a) in which half of the pentagons are not occupied by uranyl ion but by La atoms, thus the sheet obtained can be formulated $^2_\infty[La(UO_2)(VO_4)_2]^-$. The latter is deduced from the uranophane-type sheet, half of the pentagons being populated by uranyl ions and half by lanthanum ions. In the mineral ulrichite, the pentagons are half populated by uranyl and calcium ions; however the succession in the direction perpendicular to the pentagons chain

Table 4
Assignment of the bands observed on the Infra red and Raman spectra of $[La(UO_2)V_2O_7][(UO_2)(VO_4)]$.

Wave number (cm^{-1})		Vibrational mode
Infra red	**Raman**	
767–783–820	766–787	ν_1 (UO_2^{2+}) symmetric stretching
843–859–900	860–898–909	ν_3 (UO_2^{2+}) asymmetric stretching
418–453–472–549	413–431–450–516–562	ν (U–O_{eq}) equatorial vibrations
946–963	943–951	ν_1 (VO_3) symmetric stretching
713–736	711–739–753	ν_3 (VO_3) asymmetric stretching
	328–334–345–360	δ (VO_3) deformation
639	592	(V–O–V) bridges vibrations

is different leading to UO_2–PO_4–Ca–PO_4 chains [36]. Alternate of UO_2–VO_4–UO_2–VO_4 and UO_2–PO_4–M–PO_4 chains occurs for M=Pb in $Pb(UO_2)(V_2O_7)$ but, in this compound, it is limited to four chains forming four polyhedra wide ribbons rather than uranophane-type sheets [37]. Many more or less complicated geometric isomers of the uranophane-type sheet have been recognized [38]. The one observed in the $^2_\infty[La(UO_2)(VO_4)_2]^-$ layer is new and the most simple as possible: all the VO_4 tetrahedra are oriented towards the same side of the layer allowing the linkage of two parallel and inverse sheets by sharing the apical oxygen atoms O(10), to form divanadate entities V_2O_7 and double layers $^2_\infty[La(UO_2)(V_2O_7)]^{2-}$ (Fig. 3d). In these double layers a U(2)O_7 PBP is in front of a La ion, thus the uranyl oxygen O(5) is weakly bonded to La.

Finally the $^2_\infty[(UO_2)(VO_4)]^-$ sheets and the $^2_\infty[La(UO_2)(V_2O_7)]^{2-}$ double layers are alternately stacked in the [0 0 1] direction (Fig. 3e). It is noticeable that the pentagons chains of the two types of layers are perpendicular (implying that the a and b parameters are close) and the stacking puts two uranyl oxygen atoms O(1) and O(3) belonging to two U(1)O_7 PBPs and the non-shared oxygen of a V(3)O_4 tetrahedra above the La atom in opposite to O(5) assuming the cohesion of the structure through three La–O bonds and completing the coordination polyhedra of the lanthanum atom.

4.2. Thermal analysis

On heating, the DTA curve exhibits an endothermic peak at 860 °C attributed to the decomposition of $[La(UO_2)V_2O_7][(UO_2)(VO_4)]$. The XRD pattern of the cooled sample shows the presence of the two decomposition products $LaVO_4$ and $U_2V_2O_{11}$ which have formed according to the reaction:

$$LaU_2V_3O_{15} \rightarrow LaVO_4 + U_2V_2O_{11}$$

4.3. Infrared and Raman spectroscopy

To supplement this work, a study by spectroscopy Raman and Infrared was carried out (Fig. 4). The attribution of the various bands of vibration for uranyl vanadate of lanthanum $[La(UO_2)V_2O_7][(UO_2)(VO_4)]$ is carried out starting from the combination of the Infra-Red and Raman data [39].

The infrared spectrum (400–1000 cm^{-1}) of $[La(UO_2)V_2O_7][(UO_2)(VO_4)]$ is characterized by vibrations of uranyl UO_2^{2+}, vanadate VO_4 and divanadate V_2O_7 groups. For the interpretation of this spectrum the following building units have been considered: UO_2^{2+} groups, equatorial (secondary) U–O bonds in pentagonal environment, V–O–V bridges and terminal VO_3 groups (Table 4).

The bands located in the area 750–820 cm^{-1} and 850–920 cm^{-1} can be attributed to the symmetrical ν_1 and antisymmetric elongations ν_3 of UO_2^{2+}. These vibrations are in good agreement with the mathematical model suggested by Bagnall et al. [40] to determine the value of ν_1 from the one of ν_3, given by the following expression:

$$\nu_1 = 0.912\nu_3 - 1.04\ cm^{-1}$$

Thus, the application of Veal et al.'s empirical equation [41], relating bond length (R) to the asymmetric stretching vibration ν_3 (900–859–843 cm^{-1}) for uranyl groups:

$$R_{U-O(pm)} = 8120\nu_3^{-2/3} + 89.5$$

leads to the predicted uranyl bond length of 1.76, 1.79 and 1.81 Å, in good agreement with the average value obtained from X-ray structure results. The so obtained distances were compared to those found using the Bartlett et al.'s empirical equations [42] including the wavenumber values of the asymmetric ν_3 and symmetrical stretching vibration ν_1 of UO_2^{2+} obtained, respectively, from the infra-red and Raman spectra

$$R_{U-O(pm)} = 9141\nu_3^{-2/3} + 80.4$$

$$R_{U-O(pm)} = 10{,}650\nu_1^{-2/3} + 57.5$$

Table 5
Comparison of the U–O distances of $[La(UO_2)V_2O_7][(UO_2)(VO_4)]$ calculated from X-ray diffraction or from the spectroscopic data using either the Veal et al.'s or the Bartlett et al.'s equations.

U–O distances calculation Å	ν_3 (UO_2^{2+}) cm^{-1}			ν_1 (UO_2^{2+}) cm^{-1}	
	843	**859**	**900**	**766**	**787**
Veal et al.'s	1.81	1.79	1.77	–	–
Bartlett et al.'s	1.83	1.81	1.78	1.85	1.82
X-ray diffraction	1.81	1.79	1.76		

It can be seen from the values reported in Table 5 that the Veal et al.'s formulae leads to distance values closer to those found by X-ray diffraction than the Bartlett et al.'s expression.

The bands of lower intensities located in the area 400–550 cm^{-1} can correspond to the elongations of the U–O in equatorial positions in UO_2O_5. The band located around 600 cm^{-1} is allotted to the elongations of bridges V–O–V of the grouping divanadate V_2O_7. The symmetrical and antisymmetric elongations of the final VO_3 are more difficult to locate. However, the spectral zones located between 920–980 cm^{-1} and 700–750 cm^{-1}, respectively, can be attributing to them. Lastly, the bands located around 350 cm^{-1} would be due to the deformations of the final VO_3.

5. Conclusion

This work has allowed to synthesize the first lanthanum uranyl vanadate $[La(UO_2)V_2O_7][(UO_2)(VO_4)]$ by the solid state reaction using the mixed precursor of uranium and vanadium, $U_2V_2O_{11}$. The structure of $[La(UO_2)V_2O_7][(UO_2)(VO_4)]$ results from

the stacking along the *c* axis of simple layers $^{2}_{\infty}[(UO_2)(VO_4)]^{-}$ of uranophane type and $^{2}_{\infty}[La(UO_2)(V_2O_7)]^{2-}$ double layers linked by La–O bonds. In spite of numerous tentative by varying the starting materials and the experimental conditions (temperature, duration, etc.) no other lanthanide uranyl-vanadate could be synthesized by solid state reaction neither with lanthanum nor with other lanthanides. Also, due to the high stability of $LnVO_4$ preliminary formed, no lanthanide uranyl-vanadate compound could be prepared using other uranium or vanadium precursors than $U_2V_2O_{11}$.

Appendix A. supplementary material

Supplementary data associated with this article can be found in the online version at doi:10.1016/j.jssc.2011.10.042.

References

[1] P.C. Burns, M.L. Miller, R.C. Ewing, Can. Mineral. 34 (1996) 845;
P.C. Burns, Can. Mineral. 43 (2005) 1839.
[2] F. Abraham, S. Obbade, in: S.V. Elsevier, P.C. Krivovichev, Burns, I.G. Tananaev (Eds.), Structural Chemistry of Inorganic Actinide compounds, Elsevier, Amsterdam, 2007, p. 279.
[3] R. Finch, T. Murakami, Rev. Mineral. 38 (1999) 132.
[4] P.B. Barton, Am. Mineral. 43 (1958) 799.
[5] T.W. Stern, L.R. Stieff, M.N. Girhard, R. Meyrowitz, Am. Mineral. 41 (1956) 187;
F. Cesbron, J. Borène, Bull. Soc. Fr. Minéral. Cristallogr. 94 (1) (1971) 8.
[6] K. Mereiter, N. Jb. Miner. Mh. 12 (1986) 552;
F. Cesbron, N. Morin, Bull. Soc. Fr. Minéral. Cristallogr. 91 (5) (1968) 453.
[7] P. Piret, J.P. Declercq, D. Wauters-Stoop, Bull. Mineral. 103 (1980) 176.
[8] F. Cesbron, Bull. Soc. Fr. Minéral. Cristallogr. 93 (1970) 242.
[9] D.E. Appleman, H.T. Evans, J. Am. Miner. 50 (1965) 825;
F. Abraham, C. Dion, M. Saadi, J. Mater. Chem. 3 (1993) 459.
[10] I.L. Botto, E.J. Baran, Z. Anorg. Allg. Chem. 426 (1976) 321.
[11] F. Abraham, C. Dion, N. Tancret, M. Saadi, Adv. Mater. Res. (1994) 511.
[12] D.P. Shashkim, Dokl. Akad. Nauk SSSR 220 (1974) 1410.
[13] F. Cesbron, Bull. Soc. Fr. Minéral. Cristallogr. 93 (1970) 320.
[14] J. Borene, F. Cesbron, Bull. Soc. Fr. Mineral. Cristallogr. 93 (1970) 426.
[15] M. Rivenet, N. Vigier, P. Roussel, F. Abraham, J. Solid State Chem. 180 (2007) 722.
[16] M. Saadi, C. Dion, F. Abraham, J. Solid State Chem. 150 (2000) 72.
[17] C. Dion, S. Obbade, E. Rackelboom, M. Saadi, F. Abraham, J. Solid State Chem. 155 (2000) 342.
[18] S. Obbade, C. Dion, L. Duvieubourg, M. Saadi, F. Abraham, J. Solid State Chem. 173 (2003) 1.
[19] I. Duribreux, C. Dion, F. Abraham, M. Saadi, J. Solid State Chem. 146 (1999) 258.
[20] S. Obbade, C. Dion, M. Saadi, F. Abraham, J. Solid State Chem. 177 (2004) 1567.
[21] S. Obbade, C. Dion, M. Rivenet, M. Saadi, F. Abraham, J. Solid State Chem. 177 (2004) 2058;
S. Obbade, L. Duvieubourg, C. Dion, F. Abraham, J. Solid State Chem. 180 (2007) 866;
S. Obbade, C. Renard, F. Abraham, J. Solid State Chem. 182 (2009) 413.
[22] L. Jouffret, M. Rivenet, F. Abraham, J. Solid State Chem. 183 (2010) 84;
L. Jouffret, Z. Shao, M. Rivenet, F. Abraham, J. Solid State Chem. 183 (2010) 2290.
[23] N.G. Chernorukov, E.V. Suleimanov, A.V. Knyazev, E.Y. Klimov, Radiochemistry 41 (6) (1999) 515.
[24] N.V. Karyakin, E.V. Suleimanov, A.V. Knyazev, V.V. Veridusova, Russian J. Gen. Chem. 74 (5) (2004) 643.
[25] J. Rodriguez-Carvajal, Physica B 192 (1993) 55.
[26] G. Caglioti, A. Paoletti, F. Ricci, Nucl. Instrum. Methods 3 (1958) 223.
[27] SAINT Plus version 5.00, Bruker Analytical X-ray Systems, Madison, WI, 1998.
[28] G.M. Sheldrick, SHELXTL P.C., Version 6.12, An Integrated System for Solving, Refining, and Displaying Crystal Structures from Diffraction Data, Siemens Analytical X-ray Instruments Inc., Madison, WI, 2001.
[29] R.H. Blessing, SADABS, Program for absorption correction using SMART CCD based on the method of Blessing, 1995.
[30] N.E. Brese, M. O'Keeffe, Acta Crystallogr. B47 (1991) 192.
[31] P.C. Burns, R.C. Ewing, F.C. Hawthorne, Can. Mineral. 35 (1997) 1551.
[32] A.J. Locock, P.C. Burns, J. Solid State Chem. 176 (2003) 18.
[33] N. Tancret, S. Obbade, F. Abraham, Eur. J. Solid State Inorg. Chem. 32 (1995) 195;
A.M. Chippinade, P.G. Dickens, G.J. Flynn, G.P. Stuttard, J. Mater. Chem 5 (1) (1995) 141.
[34] R.D. Shannon, C. Calvo, Can. J. Chem. 51 (1973) 70.
[35] Yu.E. Gorbunova, S.A. Linde, A.V. Lavrov, A.B. Pobedina, Dokl. Akad. Nauk SSSR 251 (1980) 385.
[36] U. Kolitsch, G. Giester, Mineral. Mag. 65 (2001) 717.
[37] S. Obbade, C. Dion, M. Saadi, S. Yagoubi, F. Abraham, J. Solid State Chem. 177 (2004) 3909.
[38] L. Jouffret, M. Rivenet, F. Abraham, Mater. Sci. Eng. 9 (2010) 012028.
[39] R.L. Frost, J. Cejka, M.L. Weier, W. Martens, D.A. Henry, Vib. Spec. 39 (2005) 131.
[40] K.W. Bagnall, M.W. Wakerley, J. Inorg. Nucl. Chem. 37 (1) (1975) 329.
[41] B.W. Veal, D.J. Lam, W.T. Carnall, H.R. Hestra, Phys. Rev. B (1975) 5651.
[42] J.R. Bartlett, R.P. Cooney, J. Mol. Struct. 193 (1989) 295.